H. Sobieczky[1] , F. C. Dougherty[2] , K. Jones [3],
Dept. of Aerospace Engineering, University of Colorado, Boulder, Co.

Hypersonic Waverider Design from Given Shock Waves

INTRODUCTION

Supersonic flow elements are valuable components for the development of new aerodynamic design concepts for efficient high speed flight vehicles. Among these elements, waveriders are almost classical cases where a component may already form a high lift-overdrag (L/D) configuration [1,2]. In the past decades, the mathematical models of plane or axisymmetric supersonic flow fields with shocks have been used to create a number of simple test cases for experimental investigation, long before numerical flow analysis methods and large computers were available.

Today we have various inviscid and viscous CFD analysis methods operational to investigate the aerodynamic performance of airfoils, wings and 3D configurations in design and off-design conditions. Waveriders are ideal test cases for numerical methods simulating inviscid compressible flow: Special known shock patterns occur on relatively simple geometries at design conditions. In this situation we may think about creating more general and perhaps optimal waveriders by new design methods, mature CFD analysis will verify the predicted inviscid flows and viscous flow effects subsequently should provide performance data allowing for substantial reductions in systematic windtunnel testing.

Inverse aerodynamic design is a method to obtain configuration elements compatible with certain performance characteristics. In supersonic and hypersonic flow, the shock wave formed by the lifting body at the leading edge is carrying much of the information about lift, wave drag and noise, these are the key issues in applied supersonic aerodynamics. It seems a challenging task therefore to invert the design problem by controlling the bow shock wave and find compatible body surfaces. Waverider flows to date are simple known plane or axisymmetric flow fields, suitably cut by stream surfaces to provide special delta wings with sharp leading edges.

In this paper we try to generate waverider flows from given shock wave geometries. One approach is an approximative extension of the concept to generate waveriders from conical flows. More general shapes can thus be found by allowing the shock to have a somewhat more general shape than an axisymmetric cone.

Another way to be illustrated here is the solution of the ill-posed problem of prescribing a shock wave and finding the flow field behind it. It is stressed that ill-posedness is just a warning that standard numerical approaches may fail here, ill-posedness does not tell us the detailed reasons for it. Dealing with such problems requires the study of several supersonic flow elements. It is therefore useful to sketch some properties of such flows, the 2D and 3D wave equation proves quite useful to illustrate the approach used in the following, marching in space normal to the main flow direction.

---

1) Visiting Prof., permanent address: DLR Göttingen, Germany, 2) Asst. Prof. 3) Grad. Res. Asst.

MODELLING SUPERSONIC FLOW FIELDS WITH CROSS - MARCHING

This work is an approach to compute supersonic flowfield models which are mathematically simulating a part of the inviscid flow past an aerodynamic configuration. For waveriders, these flows will be bounded by a shock wave, a stream surface defining a solid body contour, and an exit surface. Such boundaries allow to place this model within given supersonic upstream flow conditions, connected along the shock by the Rankine - Hugoniot relations.

An earlier, similar approach [3] was aimed at connecting a local supersonic flow field with surrounding subsonic flow along a prescribed sonic line. This procedure was used to model transonic flows with applications in supercritical wing design [4]. The design process was first carried out in the hodograph plane for airfoils, where a linear method of characteristics is equivalent to marching in a direction normal to the flow ("cross - marching"), thus allowing for a start at initial conditions compatible with embedded supersonic flow domains.

Within 2D inviscid supersonic flow, a local linearization of the basic equation for a velocity potential Φ gives the wave equation

$$\Phi_{xx} - \Phi_{zz} = 0 \qquad (1)$$

where x is the direction of the local flow vector. We realize that both x and z are time-like directions, a marching in the flow direction or normal to it are mathematically equivalent, their choice determined only by formulation of the initial conditions, see Fig. 1.

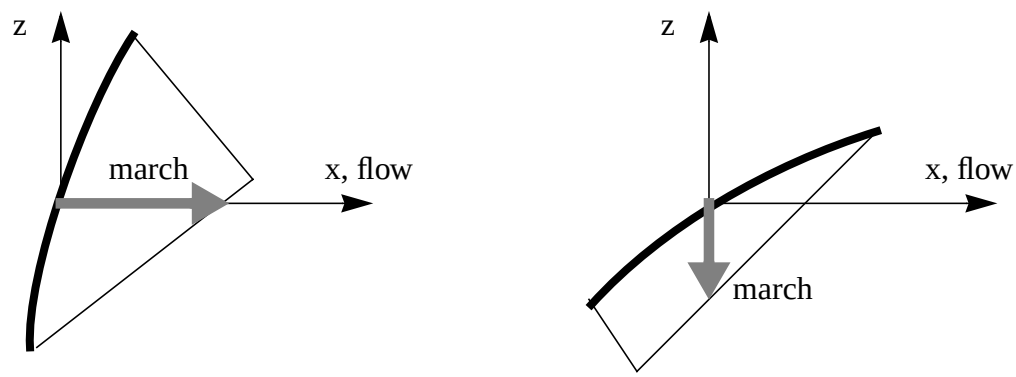

Figure 1: Initial conditions for downstream marching (a), cross - marching (b)

Axisymmetric flows are a special case of 3D flows, but their computation may also be carried out in a 2D meridional plane by the method of characteristics. It can be shown that the axisymmetric model equation for linear supersonic flow

$$\Phi_{xx} - \Phi_{rr} - \Phi_r / r = 0 \qquad (2)$$

can be used to second order approximate locally a 3D flow element which is a solution to the general 3D flow equation

$$\Phi_{xx} - \Phi_{yy} - \Phi_{zz} = 0 . \qquad (3)$$

Location of the axis of this osculating axisymmetric flow depends on local flow curvature and velocity gradient. This can be used to develop a 3D method of characteristics, which has locally 2D properties and therefore reduces perturbation amplification in a numerical cross - marching.

Figure 2 illustrates 2D flow and the possibility to locally approximate 3D flow by an axisymmetric flow model.

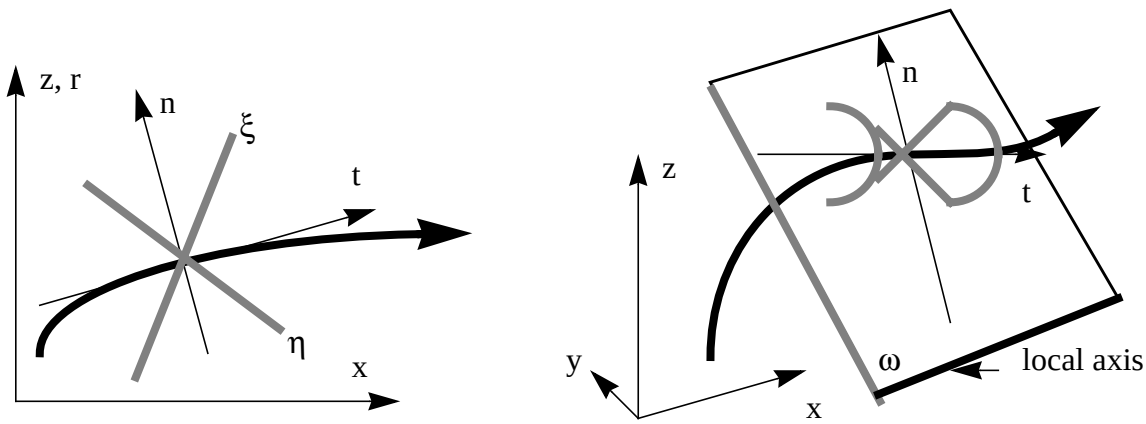

Figure 2: Two - and three-dimensional flow. Normal and tangential vectors n,t. Osculating plane ω to streamline as a meridional plane of osculating axisymmetric flow, characteristic lines ξ, η in 2D flow, Mach conoids in 3D flow.

The abovementioned description of cross - marching is intended to familiarize the reader with a strategy of numerical marching from initial data determined solely by unperturbed upstream flow and a geometrically defined oblique shock wave. The flow field behind this shock has to be evaluated by using the method of characteristics, for irrotational flow equivalent to a potential flow solver, for rotational flow resulting from an arbitrarily curved shock wave equivalent to an Euler solver. Boundaries for and from characteristics calculation in the following will be explained for the simple flow past a wedge, because using a marching code later will require to keep in mind regions of dependence if the code should work properly.

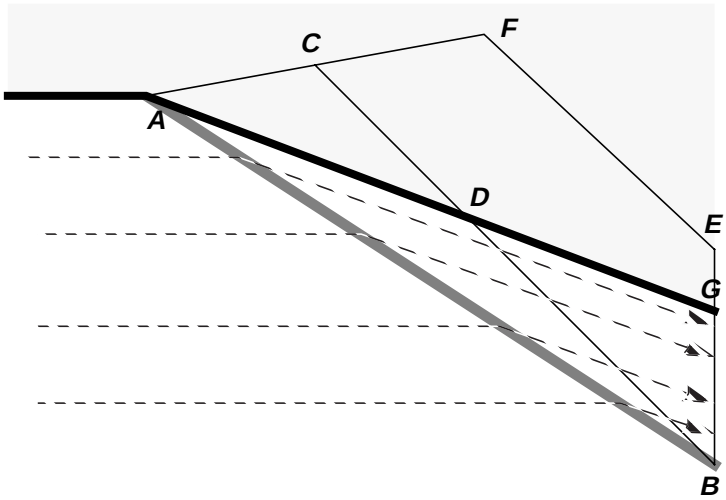

Figure 3: Supersonic flow past a wedge: Regions of dependence for cross - marching, with given shock AB and given exit BE.

The flow past a wedge is sketched in Fig. 3 to show how cross - marching will be used to obtain the flow field solution in part or in whole. Let supersonic flow be deflected by a wedge contour AG. A shock AB forms end bends the streamlines within triangle AGB conformal to the wedge angle.

We ask now for the inverse computational approach to find the flow and the contour behind the given portion AB of the shock wave. Characteristics resulting from cross - marching will define a triangular region of dependence ABC, which includes a non-physical part of the solution beyond the contour AD. On the other hand , a part DBGof the physical solution is not available with initial data given only along AB. Data need to be given also along a portion BE of the exit, with results along CB available this defines the solution within the polygon CBEF. Evaluation will define the streamline continuation beyond D toward an exit value at G. For high supersonic Mach numbers, contour part AD may be only a fraction of the continuation DG.

For curved shock waves prescribed, we have to expect rotational post-shock flow resulting from the computation. The contour streamline is another characteristic now, cross - marching requires now avoiding contradictory initial data along AB and BE, if both domains are to be solved. Furthermore, data for entropy or vorticity distribution are not defined beyond the contour (to be computed), which may pose a problem for cross - marching.

Another feature of cross - marching with the method of characteristics is the possibility of limit lines occurring in the flow computed. A multivalued solution may be computed because the marching is essentially carried out in a hodograph plane, i. e. a variable of state , for instance the velocity q , is the independent variable to march along, while coordinates

x of physical space are resulting, see Fig. 4. Such a solution cannot be obtained by marching in physical space: the marching direction would have to be reversed to pick up the continuous solution q(x). Occurrence of a limit line or surface alerts us that the given shock wave is not compatible with a smooth flow downstream of it, the initial data should be changed.

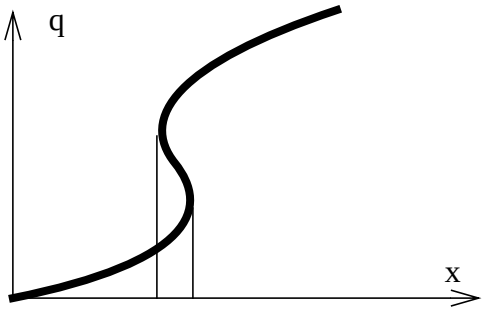

Figure 4: Representative variable of state q as a function of representative space coordinate x: multivalued solution if limit lines (surfaces) occur.

We draw some conclusions from this outline of models to be simulated numerically and used for practical design aerodynamics:

1. Given oblique shock waves require cross - marching to obtain a contour compatible with initial conditions.

2. Cross - marching in 2D plane or axisymmetric flow is effectively carried out by well - posed hodograph (inverse) methods of characteristics.

3. 3D flows may be approximated locally by (osculating) axisymmetric flow.

4. Extent of contours designed with cross - marching may be small compared to extent of the given shock wave in high Mach number supersonic flow.

5. Rotational flow constrains region of dependence to physical flow bounded by designed contour.

6. Occurence of limit surfaces requires initial data modification; inverse marching allows to pick up limit lines, direct space marching results in infinite gradients.

EXTENSION OF A CONICAL FLOW WAVERIDER CODE

Before we try to find waverider shapes resulting from arbitrary shock waves, some exercises with the method by Bowcutt et al. [5] were carried out. In fact it is our task to re design one of Bowcutt's case studies with the new inverse marching technique to be developed. This goal required some generalisations of the input, illustrated as follows.

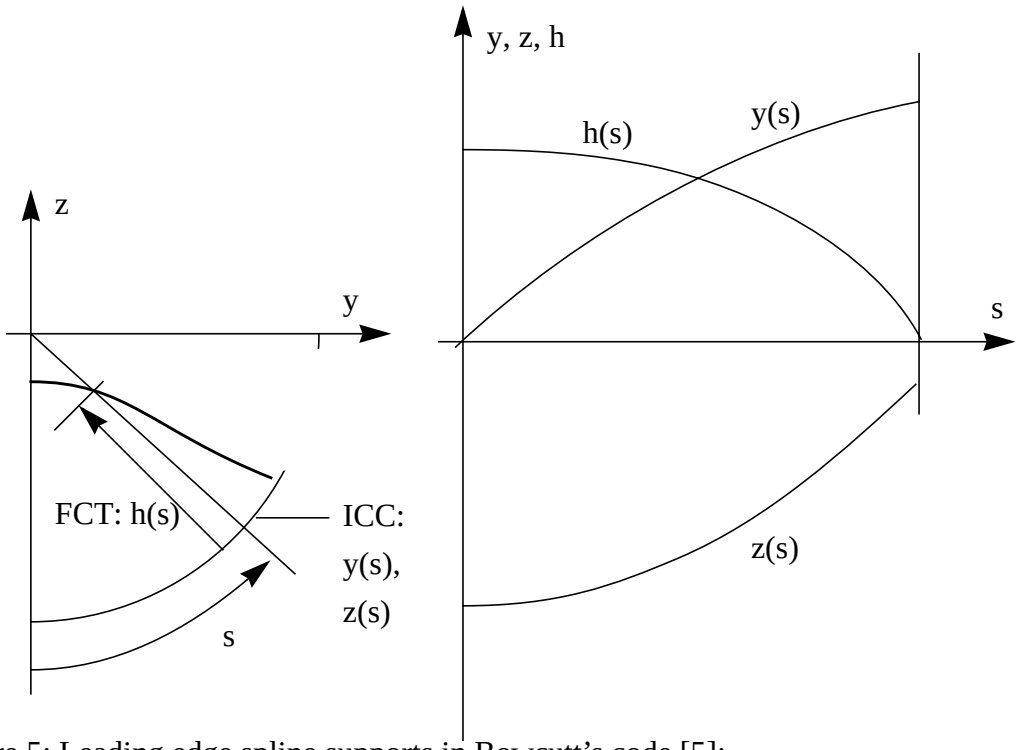

Figure 5: Leading edge spline supports in Bowcutt's code [5];
Extension: parametric functions for inlet capture curve ICC: y(s), z(s), (here: circle);
Flow capture tube FCT: h(s).

Given is a shock cone angle, the Mach number and a flow capturing tube intersecting the shock cone and thus defining the leading edge of the waverider. The computer code first integrates the Taylor - Macoll equation to model the axisymmetric conical flow field behind the shock. the leading edge is defined by a spline interpolation of given support points which in an optimization procedure are allowed to be varied for maximum lift over drag ratio. Realistic drag values are available because of solving the laminar/turbulent boundary layer equations with a correlation technique for transition prediction..

The original code defines the Flow Capturing Tube (FCT) in given Mach number supersonic flow by a set of 5 spline supports, intersecting the shock cone of given angle in axial direction. A generalisation of the given shock shape is a slope surface, with the shock angle constant but not a body of revolution anymore. This is created by an arbitrary ICC, the Inlet Capture Curve defined by y(s), z(s). The cone is easily seen as a special case here: Sine and Cosine functions for y(s) and z(s) give a circular cross section of the shock surface. The FCT is defined by the height h(s) of normals to the ICC. Very flexible functions have been included to the leading edge data generator.

A first example was intended to show that case studies by the authors of the original code can be duplicated with the new input data. Fig. 6 shows a conical flow waverider closely related to a test wing currently investigated in a NASA Langley supersonic windtunnel [6].

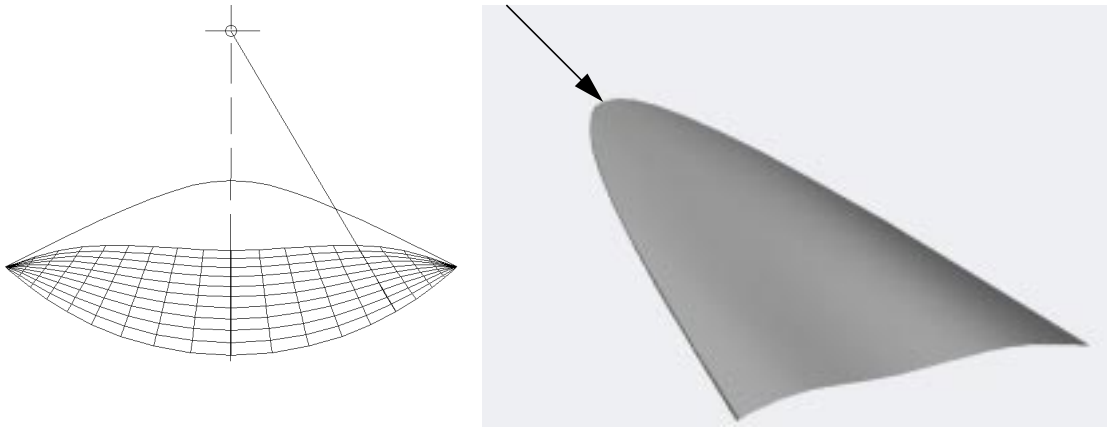

Figure 6: Conical flow waverider designed from a shock cone angle of 18 degrees, Mach = 4. Exit plane grid marks inlet area.

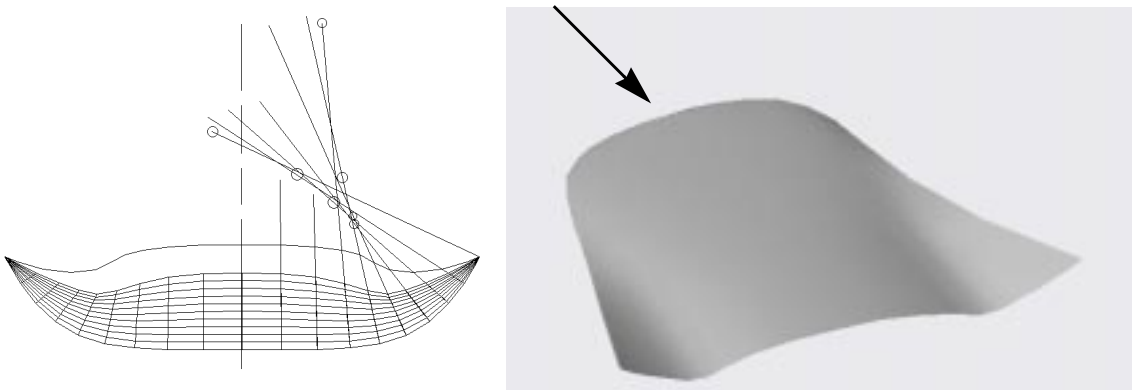

Figure 7: Osculating Cones waverider approximation designed for inlet with 2D core flow. Shock angle 18 degrees, Mach = 4. Exit plane grid marks inlet area.

Other waveriders designed include the limiting case of using 2D flow behind a plane shock wave with a parabola leading edge. This configuration can easily be described with simple analytical relations [7], also rounded leading edges can be given, using tools for general geometry generation.

Design studies with Bowcutt's method stimulated an extension to the conical flow concept which does not exploit an exact solution to the Euler equation but seems worthwhile a study nevertheless. We have noticed that prescribing a constant shock angle and an arbitrary supersonic leading edge creates a slope surface. Fig.7 shows a choice of the ICC with a flat region near the plane of symmetry, resulting in a flow largely a 2D wedge flow in the center area. Considering local flow properties behind the shock calls for using the osculating cone to the slope surface shock. The flow locally can be considered conical but with a cone axis situated in the center of curvature of the ICC. Using the present computer code we therefore evaluate conical flow streamlines scaled by local axial distance, see Fig.7.

Though the small distance between shock and surface in hypersonic flow should prove this approximative design concept not far from an exact solution, we will use CFD analysis to determine if the shock wave containment by the leading edge is to be considered satisfactory.

NUMERICAL CROSS-MARCHING FROM ARBITRARY SHOCK-WAVES

The previous chapter is intended to work toward 3D generalisations of an operational computer code, taking into account the uncertainty of doing approximations. This chapter is devoted to another, new approach which to date has been successfully verified just for a few examples. Results presented here are restricted to illustrate the procedure using the example of an analytically defined leading edge and a conical shock surface identical to the input for the example Fig. 6. We have discussed the possibility to avoid local 3D ill-posedness by marching within osculating planes. For the special conical example, these would be meridional planes, as the grid lines in Fig. 6 indicate.

Marching grid

For the purpose of experimenting with the previously outlined properties of these hyperbolic type mathematical flow models, we first neglect the osculating plane and set up a computational grid with a vertical marching direction, Fig. 8. A surface metric along the shock wave is chosen which puts a necessary grid singularity downstream to the maximum span location. Estimating the reduction of available design contour because of the triangular region of dependence (see Fig. 3) we extend the location of the exit plane downstream approximately 5 times the projected body length. The grid top layer is chosen to be very flexible, with the ultimate goal to adjust it iteratively so that the resulting contour conforms to this last step layer in the marching procedure.

Solution of the Euler Equations

Rotational, inviscid compressible flow is modelled by the Euler equations, requiring the solution for 5 variables of state: pressure, density and the 3 velocity components, represented here by a vector **f**. We have initial conditions from given shock geometry and the Rankine - Hugoniot relations. We set up the steady 3D Euler equations in non-conservative form along the initial surface, i. e. continuity, 3 momentum equations and the energy equation, to obtain a system of 5 linear equations for 15 unknown gradients (**see Appendix**):

$$A_{ij}\,\mathbf{f_x} = 0\,, \qquad i = 1, 5:\ j = 1, 15 \tag{4a}$$

where

$$\mathbf{f} = (p, \rho, u, v, w),$$

$$\mathbf{x} = (x, y, z),$$

$$A_{ij} = A_{ij}(\mathbf{f}).$$

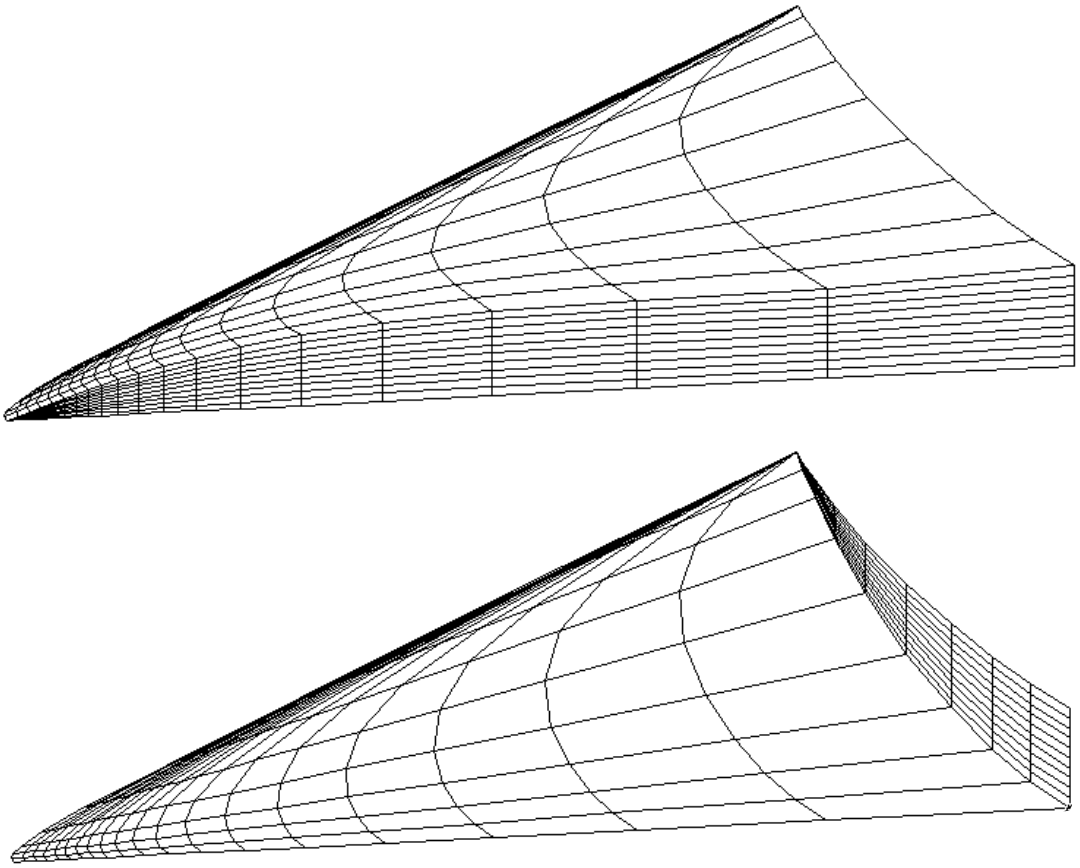

Figure 8: Grid for vertical marching from a conical shock wave. Above: Top grid layer and center plane; Below: Bottom grid layer (= shock surface) and exit plane.

Further relations are available from given variables of state along a surface in 3D space. We need the gradient of these data in both horizontal directions (x, y). Partial derivatives of $\mathbf{f}$ in 3D space are related to those of $\mathbf{f}_1 = \mathbf{f}(x, y, z_1)$ along a given surface $z_1(x,y)$ by the equations

$$\delta \mathbf{f}_1/\delta x = \mathbf{f}_x + \mathbf{f}_z\, \delta z_1/\delta x \ ,$$

$$\delta \mathbf{f}_1/\delta y = \mathbf{f}_y + \mathbf{f}_z\, \delta z_1/\delta y \ ,$$

which provide the 10 remaining equations

$$A_{ij}\, \mathbf{f_x} = B_i \ , \qquad i = 6, 15: \ j = 1, 15. \qquad (4b)$$

We solve the linear system for the unknown gradients, which allows to extrapolate the solution in any direction. As mentioned above, in this first approach we only use gradients $\mathbf{f}_z$ in the vertical direction z. Because of the analytical structure of the first grid layer, the

given shock wave, we have all partial derivatives of $\mathbf{f}_1$ and z_1 available.

The next step is using gradients $\mathbf{f}_z$ to extrapolate toward the next grid layer. We use a refined spline fit to determine the derivatives of the extrapolated function distribution. This step filters out eventual high frequency inaccuracies to be expected because of illposedness of the procedure. We use these data to solve for new gradients. The same we do with the old data on the new surface, so we have now three values for the gradient f_z , in a (z,f) - plane, see Fig. 9.

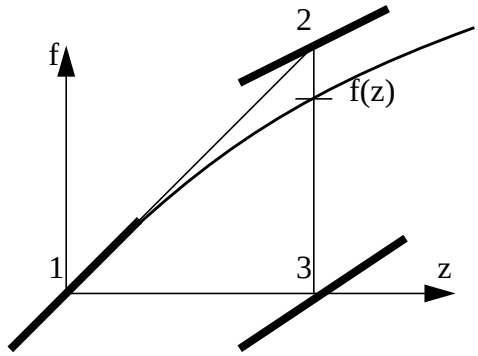

Figure 9: Local linearization of gradient distribution: Exact Differential Equation

Assuming smooth changes within this domain, (but alert to expect the occurrence of limit surfaces as illustrated in Fig. 4), we can use the three values for gradients f_z to set up locally an Exact Differential Equation

$$df/dz = a f + b z + c \qquad (5a)$$

with a, b and c determined from the three individual gradients. This O. D. E. has a solution

$$f(z) = A \exp(b z) + B z + C \qquad (5b)$$

with A, B, C easily determined from a,b,c. This determines the exact value of f at the new position z. Function f stands here for each of the five dependent variables pressure, density and the three velocity components, value z for each point of the new grid layer. After finding the horizontal derivatives of the resulting distribution we have established conditions on the new grid layer equivalent to those on the old layer and the marching process can thus be continued.

While marching, we reduce the domain observing the triangular region of dependence, Fig. 3. We use here a grid block of 20 x 10 x 11 grid points, (see Fig. 8), resulting in a reduced block of 13 x 10 x 8 points where a solution is available. This domain includes the stream surface emanating from the leading edge, as can be checked from individual

u, v, w - values along the 8th grid layer. An extrapolation to all 11 layers is carried out to ease the following streamline integration by a high accuracy postprocessing system [8].

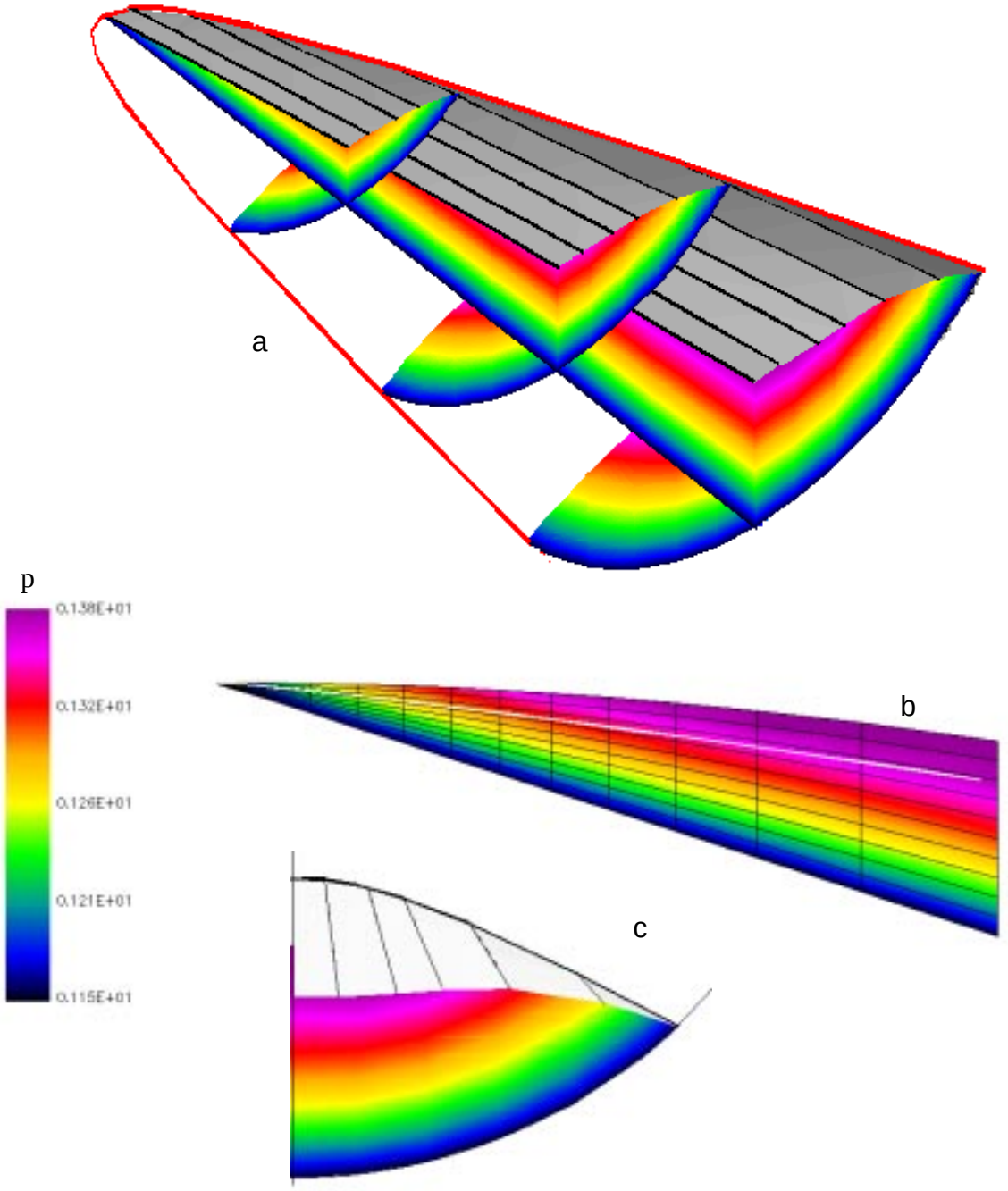

Figure 10: Results for verifying conical waverider lower surface, (compare to Fig. 6!)

(a) leading edge, color-coded isobars, integrated stream surface;

(b) grid, isobars and streamline in center plane:

(c) front view: integrated stream surface, isobars at exit plane

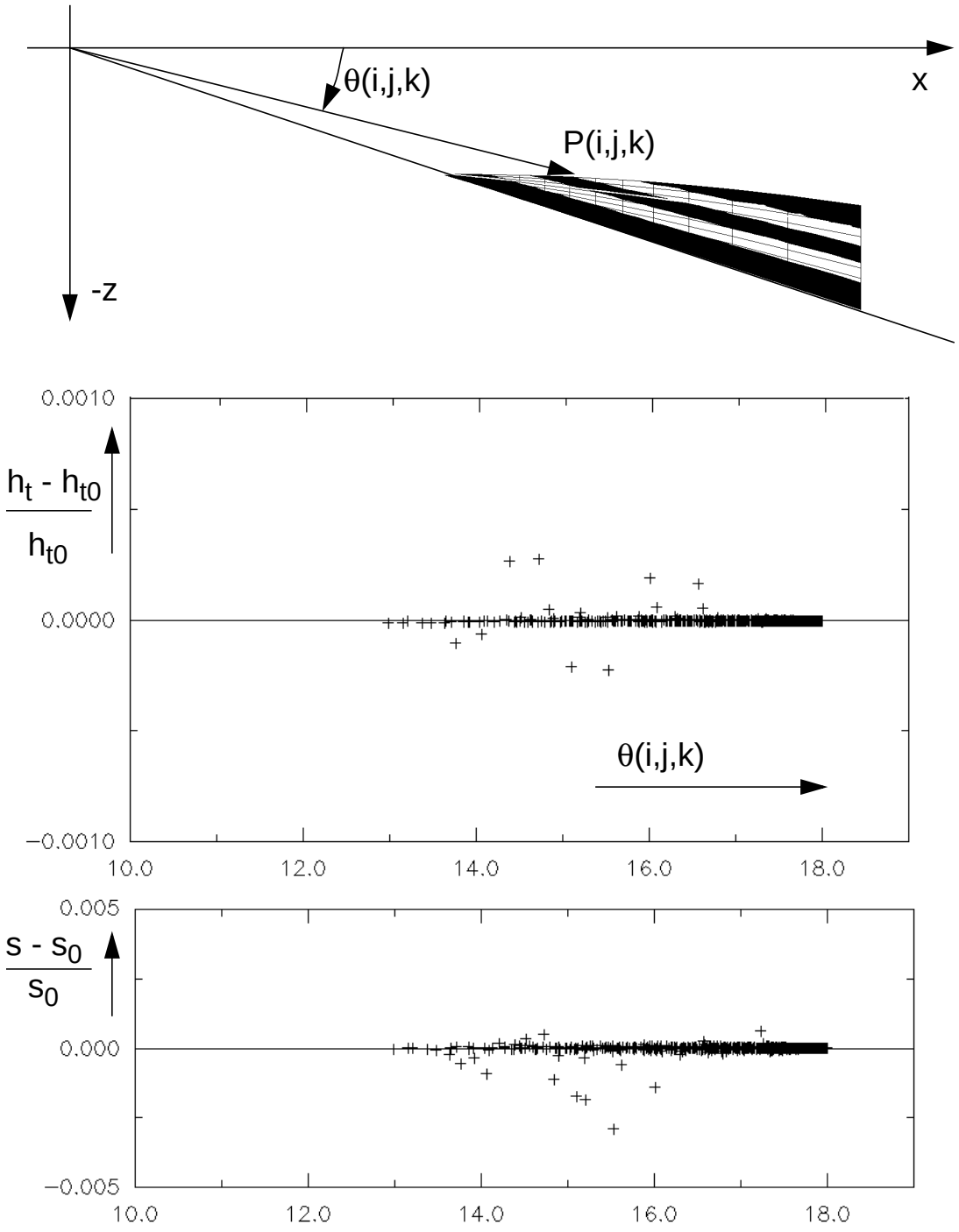

Figure 11: Verification of conical flow test example (shock angle 18 degrees):
Total enthalpy h_t and entropy s for all grid points P(i,j,k) within the flow field segment .

To check accuracy, isobar graphic visualization allows control of the conical character of this flow. Figure 10 shows results in the center plane and at several axial stations. A more rigorous test is a verification of the Taylor-Maccoll solution to this conical flow example: flow parameters on all grid points within the flow field segment are plotted against the cone angle, see Figures 11 and 12. Constant total enthalpy and entropy are found with good accuracy; pressure, density and velocity are situated along one single curve and the cross flow angle deviates less than half a degree from verifying meridional plane flow.

We have solved the Euler equations in a new inverse approach, guided by characteristic domains of dependence. The value of this method still has to be demonstrated for a variety of different case studies. It seems that this method may pave the way toward better 3D methods of characteristics to which the approach is related. For the present waverider examples, many refinements, accuracy checks and example studies - also for curved shock waves creating entropy - need to be done before this procedure may be called a valid new method to integrate the Euler equations for special flow fields like occurring behind given arbitrary oblique shock waves. The goal seems attractive: The integration with a grid size as mentioned above takes only about 2 - 3 minutes on a SUN 3-60 workstation. Taking into account various refinements and extensions to be added, this method should still be a fast procedure to integrate the steady 3D Euler equations on workstations and future PCs.

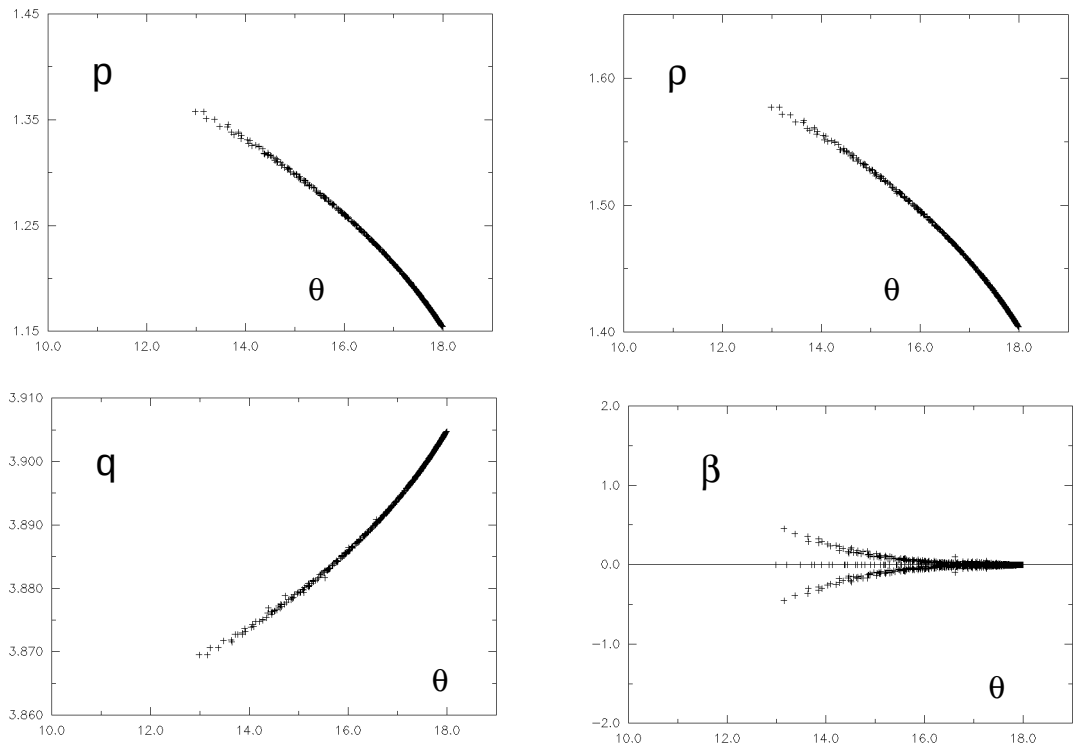

Figure 12: Verification of conical flow test example (shock angle 18 degrees): Pressure p, density rho, velocity q and meridional plane flow deviation angle β

CFD WAVERIDER ANALYSIS

In order to validate the inverse design results and analyze off-design performance of the configurations, computational methods are needed to solve both the Euler and the Navier-Stokes equations for the hypersonic simulations. Many finite difference codes have been developed for hypersonic regimes using several different computational approaches [9]. A common technique utilizes the parabolized Navier-Stokes equations such as the PNS code [10], however this method requires an initial condition which will not always be known. Another common approach applies the thin-layer approximation to the Navier-Stokes equations. This technique is used in many well-known flow solvers such as CNS [11], ARC3D [12], and F3D [13].

Code selection

ARC3D [12] incorporates a three-factored approximate factorization scheme, and solves either the Euler or the thin-layer Navier-Stokes equations in generalized coordinates for steady or time-dependent simulations. The code is fairly robust and has been used extensively in transonic and supersonic regimes. The approximate factorization scheme is inherently unstable in supersonic regimes, however, and tends to break down for Mach numbers above 3 [11]. The F3D code [13] is similar to ARC3D but includes flux-splitting in the streamwise direction. This provides a pseudo-marching scheme in one direction with a two-factored approximate factorization scheme for the other two directions. The flux splitting scheme incorporates an "upwinding" that is inherently stable in hypersonic and mixed flow regimes and requires little or no numerical dissipation. Previous work has been done with F3D for Mach numbers up to 25. The CNS code [11] is a hybrid version of the F3D code with improved boundary layer computations and an equilibrium air model. This code was still under development at the time this work effort commenced and was therefore not available. F3D was chosen as the flow solver for the validation and test phases of the inverse design effort, although several modifications had to be made to the code for Euler simulations of the waverider configurations. Sharp edges are singularities in the velocity field in inviscid analysis if stagnation is not permitted. The velocity is not defined at those points, and hence analysis at those points should be avoided. To facilitate this the surface grid points are redistributed such that the physical sharp edge is placed half way between the computational sharp edge and the adjacent surface grid points [14]. The computational leading edge is now in the flow field where the flow is defined. Adjacent values are extrapolated to the computational sharp edge in the boundary condition routines. Results generated using this technique have been quite good [15].

Test cases and results

Several test cases have been used to validate the flow solver for the waverider configurations. The F3D code was first checked for bugs in lesser-used subroutines from previous uses, and limitations to the code's performance were evaluated for the control parameters and the grid quality. The testing also provided a measure of the accuracy of the waverider solutions. The code is run on the NAS CRAY 2 and YMP and the LARC CRAY 2, and typically requires about 45 minutes for a steady state coarse grid solution (~100,000 points).

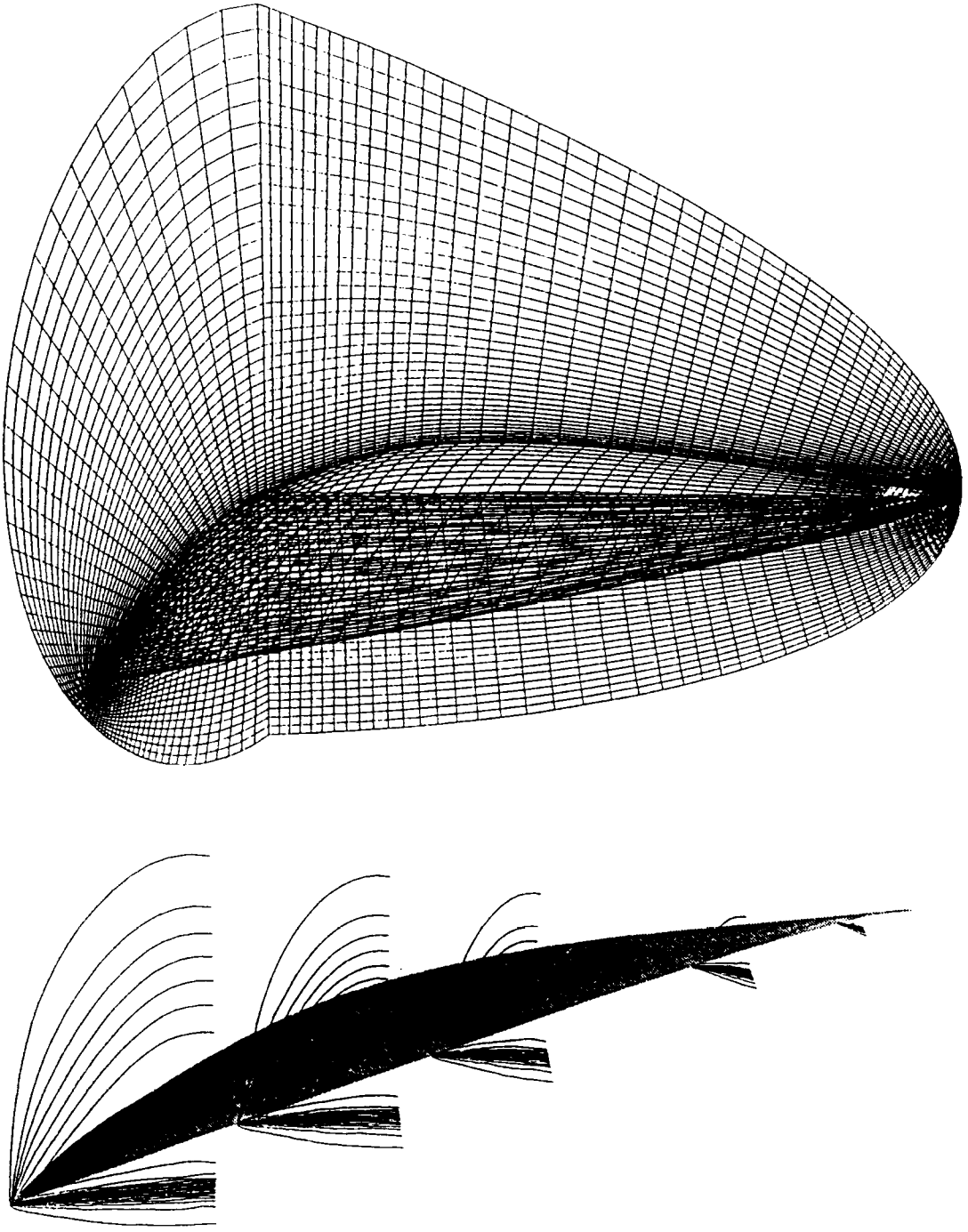

Figure 13: Inviscid analysis with F3D code: Verification of a waverider (Mach = 5.5) flow with a plane, oblique shock and an expansion on the upper surface.

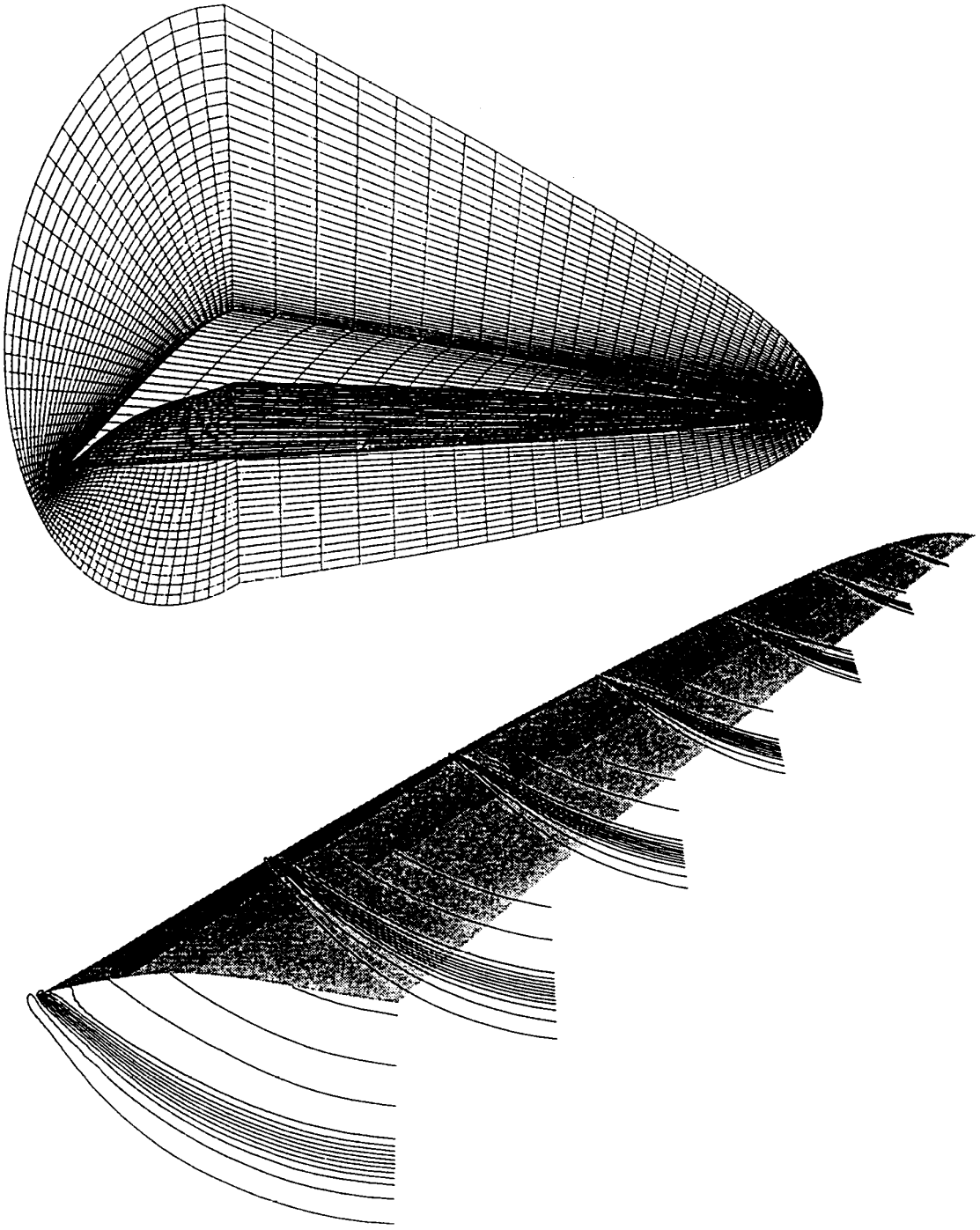

Figure 14: Inviscid analysis with F3D code: Verification of a waverider (Mach = 4) flow with a conical shock and parallel flow upper surface.

Planar Shock Waverider:

The planar shock waverider is a special case of conical waveriders where the radius of the conical shock is driven to infinity. This results in a planar shock across the lower surface of the configuration. The on-design Mach number is 5.5, and the shock angle is 17.5 degrees.
Using a newly developed grid generator, HYGRID [14], a grid was computed about the configuration. Figure 12 shows the computational grid used for the simulation and pressure contours at several cross-sections along the body respectively. The computed shock is indeed planar and the shock strength is quite accurate. The shock is smeared over roughly three grid cells and the pressure ratio across the shock is accurate to within 1% of the exact value of 2.994. The pressure contours above the waverider are caused by the Prandtl-Meyer expansion upper surface.

Conical Waveriders and Osculating Cones Configuration:

Several conical waverider test cases have been run to further validate the F3D code and our ability to produce valid solutions. An inviscid solution has been obtained for the Mach 4 waverider resulting from the extended conical flow code, Fig.6. Figure 13 shows the computational grid used for the simulation and pressure contours at various cross-sections respectively. The shock is visibly conical and attached at the leading edge. The shock is smeared over roughly 4 grid cells, and the pressure ratio across the shock is within 2% of the analytical value of 1.616. For further validation inviscid solutions for two other conical waverider shapes have been run, corresponding to wind tunnel models being tested at NASA Langley. Navier-Stokes simulations will be run on these providing a measure of accuracy for the Navier-Stokes solver.
Some encouraging inviscid analysis results have been obtained also for the non-conical design example illustrated in Fig. 7. We observe shock containment at the leading edge not only along the wedge-like front part but all the way back to the fin-like tips. A detailed description of design variations and CFD analysis of this configuration will be presented in a forthcoming report [16].

CONCLUSIONS

Two methods are presented here to obtain super/hypersonic waverider shapes with geometries more general than available from plane or axisymmetric known flow fields:

In the first approach we have made use of axisymmetric flows to construct more general flows with the new concept of "Osculating Cones". Conical waverider design can thus be extended to yield results also for shocks forming a slope surface. A relatively simple generalization of an operational conical waverider design code gives first results. Though an approximation, the concept seems to be fully confirmed by the first results of CFD analysis; further design examples will be used to find the limits of this approach. Also, axisymmetric methods of characteristics with rotation from curved shock waves will be applied in the local osculating plane: this will be a further generalization of this concept.

Cross-marching, an exact method of characteristics for inverse 2D calculations, becomes ill-posed in general 3D flow modelling. A new numerical marching technique to solve the Euler equations makes use of some features of characteristic cross-marching, first results were obtained for redesigning a given conical flow example without using conicity for the solution algorithm. Accuracy seems to be very satisfactory but many more case studies need to be done to confirm the value of this new approach. Once fully developed, the advantage of this method will be the option to define leading edges and contained shock surfaces from very flexible geometry tools, which should include parameters to find waverider and inlet configurations with optimum aerodynamic performance.

Inviscid analysis of the designed shapes was carried out to date with the F3D code. Several refinements and adaptations of this code to handle sharp leading edges had to be made. The plane and conical flow test cases were used to show the usefulness of the code. Analysis results have confirmed the Osculating Cone design approach, shock containment is verified very well. Viscous flow analysis is the logical next step, allowing for realistic lift and drag prediction.

REFERENCES

1. Kuechemann, D., "The Aerodynamic Design of Aircraft".
Oxford: Pergamon Press, (1978)

2. Anderson, J. D., "Hypersonic and High Temperature Gas Dynamics",
New York: McGraw Hill Book Company, (1989)

3. Sobieczky, H., Yu, N. J., Fung, K-Y., Seebass, A.R.,
"New Method for Designing Shock-free Transonic Configurations".
AIAA Journal Vol. 17. No. 7, pp722 - 729. (1979).

4. Sobieczky, H., Seebass, A. R., "Supercritical Airfoil and Wing Design",
Ann. Rev. Fluid. Mech. Vol. 16, pp. 337 - 63, (1984)

5. Bowcutt, K., G., Anderson, J. D., Capriotti, D.,
"Viscous Optimized Hypersonic Waveriders", AIAA paper 87-0272, (1987).

6. Bauer, S. X., "Analysis of Two Viscous Optimized Waveriders",
Proc. 1st Int. Hypersonic Waverider Symposium, Univ. of Maryland, (1991).

7. Sobieczky, H., Stroeve, J. C., "Generic Supersonic and Hypersonic Configurations",
AIAA-paper 91-3301 (1991)

8. Pagendarm, H.-G., "HIGHEND, A Visualization System for 3D Data with
Special Support for Postprocessing of Fluid Dynamics Data", Proc. Eurographics
Workshop on Visualization in Scientific Computing, Springer, (1991)

9. Deiwert, G. S. and Green, M. J., "Computational Aerothermodynamics", AAS paper 86-350, (1986).

10. Lawrence, S. L., Chaussee, D. S., and Tannehill, J. C., "Application of an Upwind Algorithm to the Three-Dimensional Parabolized Navier-Stokes Equations", AIAA paper 87-1112, (1987).

11. Flores, J., Ryan, J. S., and Edwards, T. A., "CNS Code Development", Paper 12, Fifth National Aero-Space Plane Technology Symposium, Hampton, VA, October 18-21, 1988.

12. Pulliam, T. H., "Euler and Thin Layer Navier-Stokes Codes: ARC2D, ARC3D", Computational Fluid Dynamics User's Workshop, The University of Tennessee Space Institute, UTSI Publication No. E02-4005-023-84, (1984).

13. Steger, J. L., Ying, S. X., and Schiff, L. B., "A Partially Flux Split Algorithm for Numerical Simulation of Compressible Inviscid and Viscous Flow", Proceedings of the Workshopheld by the Institute of Nonlinear Sciences, University of California, Davis.

14. Jones, K. D. and Dougherty, F. C., "HYGRID: Grid Generation for Waveriders with Sharp Leading Edges", published as a NASA CR, (1990).

15. Jones, K. D. and Dougherty, F. C., "Computational Simulation of Flows About Hypersonic Geometries with Sharp Leading Edges", AIAA paper 90-3065, (1990)

16. Center, K., Sobieczky, H., Dougherty, F. C., " Interactive Design and Analysis of Hypersonic Waverider Geometries", AIAA paper 91-1697, (1991).

ACKNOWLEDGEMENTS

This work was funded by NASA under Research contract NAG 1 - 880 and supported by DLR German Aerospace Research Establishment, Institute for Theoretical Fluid Mechanics basic funds.

Appendix:

Coefficients Matrix of the 15 Euler - Gradient equations (4)

$$A_{ij}\,\mathbf{f_x} = B_i$$

	A_{ij}															B_i
i	ρ_x	ρ_y	ρ_z	p_x	p_y	p_z	u_x	u_y	u_z	v_x	v_y	v_z	w_x	w_y	w_z	
1	u	v	w	.	.	.	ρ	.	.	.	ρ	.	.	.	ρ	.
2	u^2	uv	uw	1.	.	.	2ρu	ρv	ρw	.	ρu	.	.	.	ρu	.
3	uv	v^2	vw	.	1.	.	ρv	.	.	ρu	2ρv	ρw	.	.	ρv	.
4	uw	vw	w^2	.	.	1.	ρw	.	.	.	ρw	.	ρu	ρv	2ρw	.
5	$q^2/2$	$q^2/2$	$q^2/2$	γ/(γ-1)	γ/(γ-1)	γ/(γ-1)	ρu^2+H	ρuv	ρuw	ρuv	ρv^2+H	ρvw	ρuw	ρvw	ρw^2+H	.
6	1.	.	z^*_x	.	.	.	.	.	.	.	.	.	.	.	.	ρ^*_x
7	.	1.	z^*_y	.	.	.	.	.	.	.	.	.	.	.	.	ρ^*_y
8	.	.	.	1.	.	z^*_x	.	.	.	.	.	.	.	.	.	p^*_x
9	.	.	.	.	1.	z^*_y	.	.	.	.	.	.	.	.	.	p^*_y
10	.	.	.	.	.	.	1.	.	z^*_x	.	.	.	.	.	.	u^*_x
11	.	.	.	.	.	.	.	1.	z^*_y	.	.	.	.	.	.	u^*_y
12	.	.	.	.	.	.	.	.	.	1.	.	z^*_x	.	.	.	v^*_x
13	.	.	.	.	.	.	.	.	.	.	1.	z^*_y	.	.	.	v^*_y
14	.	.	.	.	.	.	.	.	.	.	.	.	1.	.	z^*_x	w^*_x
15	.	.	.	.	.	.	.	.	.	.	.	.	.	1.	z^*_y	w^*_y

where "." stands for zero and $H = \gamma/(\gamma-1)\,p + \rho\,q^2/2$.